Electron dynamics in vacancy islands: Scanning tunneling spectroscopy on Ag(111)

H. Jensen, J. Kröger,* and R. Berndt
Institut für Experimentelle und Angewandte Physik, Christian-Albrechts-Universität zu Kiel, D-24098 Kiel, Germany

S. Crampin†
Department of Physics, University of Bath, Bath BA2 7AY, United Kingdom
(Received 1 November 2004; revised manuscript received 7 February 2005; published 26 April 2005)

The dynamics of Ag(111) surface state electrons confined to nanoscale hexagonal and triangular vacancy islands are investigated using scanning tunneling spectroscopy. The lifetimes of quantized states with significant amplitude near the centers of the vacancies are weakly affected by the geometry of the confining cavity. A model that includes the dependence of the lifetime on electron energy, vacancy size, step reflectivity, and the phase coherence length describes the results well. For vacancy islands with areas in the range of $\approx 40-220$ nm^2 lossy scattering is the dominant lifetime-limiting process. This result and a corrected analysis of published experimental data improve the consistency of experimental and calculated surface-state lifetimes.

DOI: 10.1103/PhysRevB.71.155417 PACS number(s): 73.20.At, 72.10.Fk

Spectacular real-space observations of electron confinement have been realized by scanning tunneling microscopy (STM) and scanning tunneling spectroscopy (STS) for the Shockley-type electronic surface states on the (111) surfaces of the noble metals. The confinement of electrons to artificial (e.g., Refs. 1–5) and natural (e.g., Refs. 6–9) nanostructures has been studied in some detail. Moreover, several reports have addressed the lifetime of surface state electrons, as deduced from the tunneling spectroscopy of large terraces and scattering patterns near steps and in confining structures.[5,6,10–12] Currently, however, the influence of the confinement on electronic lifetimes is not clear.

Using low-temperature STS of triangular and hexagonal vacancy islands and model calculations, we investigate the effects of the geometry of the confining resonator and of lossy scattering at its boundary on the lifetimes of confined states. For the states investigated, which have an antinode at the center of these resonators, we find similar lifetimes independent of the geometry. The lossy scattering at the confining step edges turns out to be the lifetime-limiting process.

The experiments were performed in an ultrahigh vacuum (base pressure 1×10^{-8} Pa) at 9 K using a custom-made microscope. The tungsten tips and Ag(111) were prepared by argon ion bombardment and annealing. The hexagonal vacancy islands were fabricated by briefly (2–3 s) exposing freshly prepared Ag(111) surfaces to a low-flux argon ion beam.[13] The resulting nanostructures are shown in Fig. 1. The triangular vacancy islands were obtained through controlled tip-sample contacts. The differential conductivity (dI/dV) was measured by superimposing a sinusoidal voltage modulation (3 mV_{rms}, 10 kHz) on the tunneling voltage and measuring the current response by a lock-in amplifier.

The maps of dI/dV from a hexagonal vacancy island [Fig. 2(a)] exhibit strongly voltage-dependent features, similar to those found from, e.g., hexagonal Ag islands.[6,8] For voltages below the Ag(111) surface-state band edge at $E_0\approx-67$ mV the interior of the vacancy island is featureless, while at higher voltages increasing numbers of sixfold azimuthally symmetric rings occur. The sixfold modulation is partially distorted due to deviations of the vacancy island from a perfect hexagonal shape. With dI/dV being related to the local density of states,[14] the interference patterns are attributed to surface-state standing waves confined by scattering at the edges of the island. Figure 2(b) shows similar data for a triangular vacancy island. Starting from a featureless interference pattern at −60 mV, increasingly complex patterns occur at higher voltages. The number of antinodes increases with higher voltages, as expected from a particle-in-a-box model. At −20 mV, for instance, six antinodes of the local density of states are clearly visible.

For a quantitative measure of the confinement we acquired dI/dV spectra above the vacancy island centers. A typical spectrum of a hexagonal island [Fig. 3(a)] is comprised of a series of peaks with the first appearing just above the lower band edge of the Ag(111) surface state. The peak width increases with increasing energy. These peaks correspond to the energy levels of the confined Ag(111) surface-state electrons, with the broadening into resonances as a result of single-particle scattering processes,[2,15] many-body interactions,[16] and instrumental effects such as the finite modulation voltage and finite temperature. We have confirmed this interpretation using the same approach as in Refs. 6 and 8 using a variational embedding technique[17] to compute the electronic structure of two-dimensional electrons

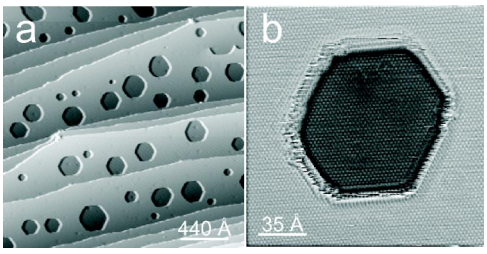

FIG. 1. (a) Constant-current STM image of Ag(111) surface after low-flux Ar^+ bombardment (200 mV, 2 nA). (b) An atomically resolved vacancy island which serves as the cavity for electron confinement.

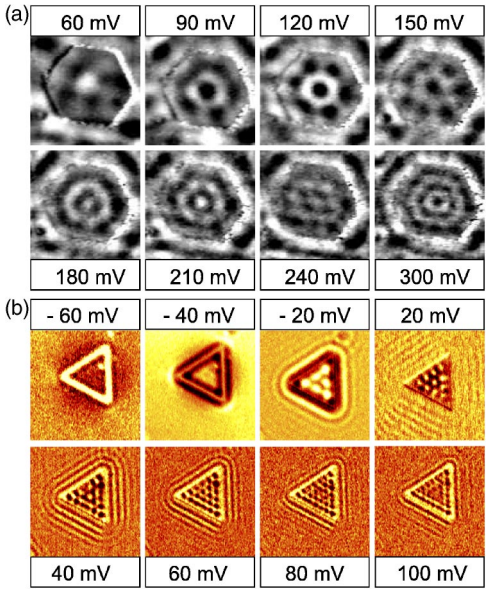

FIG. 2. (a) Series of constant-current dI/dV maps of a hexagonal vacancy island with an edge length of ≈5.8 nm recorded at the indicated sample voltages (white corresponds to large dI/dV). (b) The analogous data for a triangular vacancy with an edge length of 22 nm. For the hexagons (triangles) the feedback loop was opened at 0.5 nA (2nA) and at the indicated voltage.

with the effective mass m^* confined to hexagonal or triangular domains by an infinite barrier. This gives a series of discrete levels at energies that are dependent upon the size and geometry of the confined region, which we broaden by including an empirically determined self-energy $\mathrm{Im}\,\Sigma \approx 0.2(E - E_F)$, where E_F is the Fermi energy. Note that in comparing

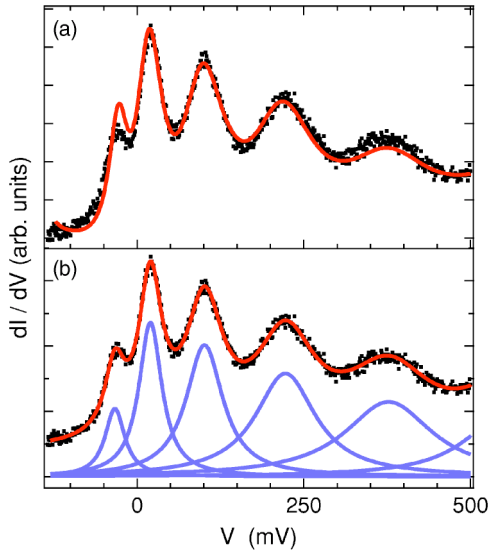

FIG. 3. (a) Experimental dI/dV data (dots) fitted by the calculated spectrum (full line) based on a variational calculation, as explained in the text. (b) The experimental dI/dV spectrum (dots) fitted by superposition of Lorentzians (full lines). The topographic edge length of the hexagonal island is 7.4 nm. The feedback loop was opened at 1 nA and 300 mV.

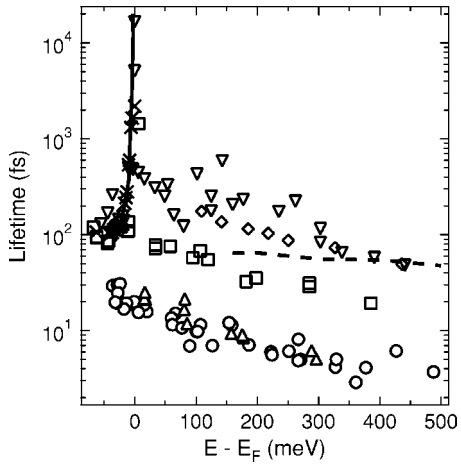

FIG. 4. Lifetime versus binding energy $E - E_F$ found for Ag(111) surface-state electrons confined to vacancy hexagons (○), vacancy triangles (△), triangular corrals of Ag adatoms (▽, from Ref. 5), circular and rectangular corrals of Mn adatoms (□, from Ref. 4); lifetimes extracted from standing wave patterns near step edges (◇, adapted from Refs. 11 and 12); photoemission data (×, from Ref. 22); results of theory are depicted as a full and a dashed line (from Refs. 22 and 12, respectively).

the experimental data with calculated spectra the true dimensions of the island must be determined. It is not *a priori* clear that the relevant dimension of the island coincides with its apparent topographic boundaries. For example, due to the finite spatial extension of the tip the topographic dimensions are expected to be smaller than the actual ones. Consequently, we fit the experimental dI/dV curves by calculated spectra, varying the edge length as the only fit parameter. The full line in Fig. 3(a) depicts the result of this fit procedure applied to the vacancy island with a topographic edge length of 7.4 nm. The fit parameter, however, is given by 7.6 nm. Performing this fit procedure for several island sizes, we find that the topographs of the vacancy islands tend to underestimate the actual sizes.

We now discuss the lifetimes of the quantized electron states, which are proportional to the inverse width of the associated peaks in the dI/dV spectra. In particular the half width at half maximum (HWHM) of the electron levels corresponds to an energy uncertainty ($\mathrm{Im}\,\Sigma$) related to the lifetime τ of the electronic state via

$$\tau = \hbar/(2\ \mathrm{Im}\,\Sigma) \approx 329\ \mathrm{meV\ fs/Im}\,\Sigma. \qquad (1)$$

In analyzing the peak width, the instrumental broadening due to voltage modulation and thermal effects have been taken into account. A fit using five Lorentzians plus an additional one at high energies to match the background is shown in Fig. 3(b). Taking the HWHM of the Lorentzians we arrive at the corresponding imaginary parts of the self-energy, which is converted to a lifetime using Eq. (1). Figure 4 displays the electronic lifetimes versus their binding energies, as extracted from various hexagonal (circles) and triangular (triangles) vacancy islands, along with the original data from several other Ag(111) surface-state-lifetime studies, both ex-

perimental and theoretical. While a general trend of increasing lifetime as the binding energy approaches the Fermi level is obvious (due to the vanishing of electron-electron and electron-phonon scattering as $|E-E_F|\rightarrow 0$),[19] there are significant differences in magnitudes, to be discussed next.

We first note from the vacancy data of Fig. 4 that the geometric shape of the confining structure has little impact on lifetimes. Consequently, in modeling, we consider a *circular* vacancy island where the high symmetry permits a relatively simple description. In particular, one can show[18] that the confined levels occur at energies for which

$$Re^{2ikS}e^{-S/L_\Phi}e^{-i\pi/2}=1. \tag{2}$$

S is the radius of the vacancy, $k=\sqrt{2m^*(E-E_0)/\hbar^2}$ is the magnitude of the surface electron wave vector, and R is the reflection coefficient describing scattering from the confining atomic step. Equation (2) is similar to the round-trip phase condition for surface states in the phase-accumulation model,[20,21] where electrons undergoing multiple reflections at barriers with reflection coefficients R_l and R_r separated by distance d are found at energies given by $R_lR_r\exp 2ikd=1$. In the vacancy island the round trip corresponds to starting and finishing at the center, and it only involves one reflection—so just one reflection coefficient appears in Eq. (2)—and in the vacancy island the wave function must have an antinode at the center to be visible in STS, so that the round-trip phase corresponds to an odd number of half wavelengths. This is the effect of the $\exp -i\pi/2$ factor in Eq. (2). One final difference is that Eq. (2) also takes into account many-body interactions through the factor containing L_Φ, the phase-relaxation length due to electron-electron (*e-e*) and electron-phonon (*e-p*) scattering. L_Φ is related by the group velocity $v_g=\hbar k/m^*$ to the corresponding inelastic scattering lifetime τ_I; $L_\Phi=v_g\tau_I$.

Writing $R=\exp i(\phi_R-i\ln|R|)$, Eq. (2) is satisfied when

$$\phi_R-i\ln|R|+2kS+iS/L_\Phi-\pi/2=2\pi n, \tag{3}$$

for $n=1,2,\ldots$, which has solutions at the complex energies $E-i\,\mathrm{Im}\,\Sigma$. Assuming $\mathrm{Im}\,\Sigma\ll(E-E_0)$, the real and imaginary parts of Eq. (3) give the energy of the nth level,

$$E_n=E_0+\frac{\hbar^2(n\pi+\pi/4-\phi_R/2)^2}{2m^*S^2}, \tag{4}$$

and corresponding width,

$$\mathrm{Im}\,\Sigma_n=\frac{\hbar v_g}{2}\left[-\frac{\ln|R|}{S}+\frac{1}{L_\Phi}\right], \tag{5}$$

where v_g, $|R|$, and L_Φ are evaluated at the energy E_n. Hence the lifetime of the surface-state electrons confined within the vacancy islands is given by

$$\tau^{-1}=\tau_R^{-1}+\tau_I^{-1}, \tag{6}$$

where the lifetime τ_R associated with lossy scattering at the atomic step is

$$\tau_R=-\frac{S}{v_g\ln|R|}. \tag{7}$$

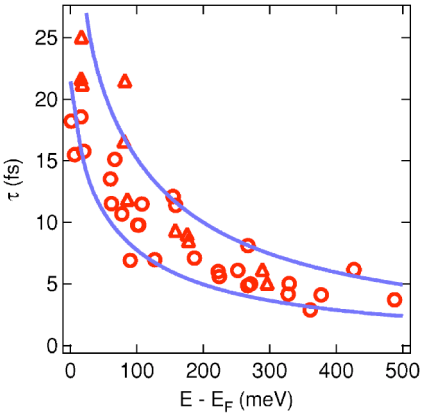

FIG. 5. Lifetime data for Ag(111) surface state electrons confined to hexagonal (○) and triangular (△) vacancy islands together with calculated values (full lines) for the smallest ($R=4$ nm, lower curve) and largest ($R=8.5$ nm, upper curve) islands investigated.

At 225 meV, Vitali *et al.*[12] find $\tau_I\approx 62$ fs in calculations that include the surface band structure and which treat *e-e* interactions within the GW approximation[10] and use the full Eliashberg spectral function for the *e-p* interaction.[22] Bürgi *et al.*[7] have measured the reflection coefficient for surface-state scattering at ascending steps on Ag(111) and report $|R|\approx 0.23\pm 0.07$ at 225 meV. Using Eq. (7) (and $m^*=0.42m_e$),[6] this gives $\tau_R\approx(9\pm 2)$ fs for an island with edge of 7.5 nm, and from Eq. (6) it gives a lifetime of $\tau\approx(7.9\pm 1.5)$ fs. This is consistent with our measured lifetimes shown in Fig. 4. The calculated result is exemplary for the overall consistency with our measured lifetime data. We can therefore conclude that at this energy the electron states within the vacancy island are roughly 8 times more likely to decay via lossy scattering at the confining boundary than via inelastic *e-e* and *e-p* scattering. In Fig. 5 we plot the lifetime, τ, versus the binding energy, $E-E_F$, for all sizes of vacancy islands studied (circles and triangles). The full lines are calculated from Eq. (6), using Eq. (7) for τ_R and the theoretical data from Refs. 12 and 22 for τ_I. The upper (lower) curve was calculated for an island size of $S=8.5$ nm ($S=4.0$ nm), which reflects the edge length of the largest (smallest) island investigated in our study. Our experimental data are bounded above and below by the calculated curves, revealing that our analytical model gives reasonable results. As a consequence we find that the lossy boundary scattering is the dominant lifetime-limiting process for all islands that we have studied. They would need to be typically 1 order of magnitude larger in dimension for the inelastic *e-e* and *e-p* scattering to become dominant.

Bürgi *et al.*[7] find that $|R|$ decreases with increasing energy. Using their values, we find that $-\ln|R|$ varies approximately as $(E-E_0)^{1/2}$. Since $v_g\propto(E-E_0)^{1/2}$ and since L_Φ^{-1} is negligible with respect to $\ln|R|/S$ in Eq. (5) due to the dominance of the lossy-scattering mechanism, the level width increases approximately linearly with energy. A similar variation in level width was previously inferred by Li *et al.*[6] for surface-state confinement to adatom islands, where a phenomenological self-energy $\mathrm{Im}\,\Sigma=0.2(E-E_0)$ was found to match the observed level broadening. Bürgi *et al.*[7] have shown that the

reflection coefficient for the descending steps, which surround the adatom islands, varies in a similar manner to that for the ascending steps.

In Fig. 4 various other lifetime data are shown. The Mn corral values obtained by Kliewer *et al.*[4] (□) have been obtained by analyzing experimentally determined spectral linewidths, using the two-dimensional "black-dot" scattering model introduced by Heller *et al.*[2] The lifetime is obtained using Eq. (1) where $\mathrm{Im}\,\Sigma$ is the electron self-energy needed to bring the calculated spectra into agreement with the measured ones. In effect, the lifetime is assumed to be due to *e-e* and/or *e-p* scattering, and hence to be identified as τ_I, as the scattering properties of the confining adatom array are incorporated via the multiple-scattering equations. However, the nature of the system is similar to the present one, with the total linewidth being a sum of the contributions due to lossy scattering and the *e-e* and/or *e-p* scattering. Hence the assumption that Mn adatoms act as black-dot scatterers means that the lifetime values that have been obtained should be viewed as lower limits to τ_I. The true reflectivity of the Mn adatom corrals is likely to be lower than that of the assumed black-dot scatterers, meaning that the lossy scattering is actually greater than modeled. Hence a smaller amount of the measured linewidth should be attributed to *e-e* and/or *e-p* scattering, increasing τ_I.

The lifetimes deduced from the decay of the standing wave patterns at steps for the image-potential states[23] and surface states[11,12] (the latter are depicted as diamonds in Fig. 4) are not complicated by lossy scattering as the asymptotic decay of the standing waves depends only upon τ_I. However, Wahl *et al.*[23] and Bürgi *et al.*[11] have misidentified the correct dependence of the standing wave patterns on the phase-coherence length, so that their lifetimes are actually twice τ_I.[24] The lifetimes determined by Braun and Rieder[5] shown in Fig. 4 (▽) have been obtained from a detailed analysis of the standing wave patterns in triangular corrals constructed from Ag adatoms. In their analysis the Ag adatoms are not treated as black-dot scatterers, but as point scatterers whose scattering properties are determined by fitting, along with a phase-coherence length which enters an attenuation factor $\exp -r/\tilde{L}_\Phi$ in the electron propagation over a distance r between scattering events, and to and from the STM tip position. Thus the lossy scattering effects are fully accounted for in this work—insofar as the two-dimensional point-scatterer model is valid—but the attenuation factor used is based upon the incorrect phase-coherence dependence described by Bürgi *et al.*[11] so that again an incorrect relationship is used between the phase-coherence length $\tilde{L}_\Phi$ and the lifetime τ_I. We have shown that $\tilde{L}_\Phi$ is twice as large as the correct phase-coherence length L_Φ.[18] As a consequence, the published lifetimes[5] must be halved. Correcting for this, the agreement between the lifetimes found by Braun and Rieder and the theoretical values for Ag(111), which are generally lower than those found in Ref. 5, is improved.

In summary we have investigated the lifetimes of electrons confined to vacancy islands with areas $\approx 40-220$ nm^2 on Ag(111). We find that the geometry of the vacancy has only a weak influence on the lifetimes, which are dominated by lossy scattering at the steps which form the edges of the island. The lifetimes are well described by a theory that includes the dependence on the electron energy, vacancy size, step reflectivity, and the phase-coherence length. This indicates that the crossover to lifetimes dominated by electron-electron and electron-phonon scattering will occur for islands with dimensions of 1 order of magnitude greater than those studied here. This result and a corrected analysis of published experimental data lead to a more consistent picture of surface-state lifetimes in experiments and calculation.

H. J., J. K., and R. B. thank the Deutsche Forschungsgemeinschaft for financial support. S. C. acknowledges the support of the British Council.

*Electronic address: kroeger@physik.uni-kiel.de
†Electronic address: s.crampin@bath.ac.uk

[1] M. F. Crommie, C. P. Lutz, and D. M. Eigler, Science **262**, 218 (1993).
[2] E. J. Heller, M. F. Crommie, C. P. Lutz, and D. M. Eigler, Nature (London) **369**, 464 (1994).
[3] J. Kliewer, S. Crampin, and R. Berndt, Phys. Rev. Lett. **85**, 4936 (2000).
[4] J. Kliewer, R. Berndt, and S. Crampin, New J. Phys. **3**, 22 (2001).
[5] K.-F. Braun and K.-H. Rieder, Phys. Rev. Lett. **88**, 096801 (2002).
[6] J. Li, W.-D. Schneider, R. Berndt, and S. Crampin, Phys. Rev. Lett. **80**, 3332 (1998).
[7] L. Bürgi, O. Jeandupeux, A. Hirstein, H. Brune, and K. Kern, Phys. Rev. Lett. **81**, 5370 (1998).
[8] J. Li, W.-D. Schneider, S. Crampin, and R. Berndt, Surf. Sci. **422**, 95 (1999).
[9] I. Barke and H. Hövel, Phys. Rev. Lett. **90**, 166801 (2003).
[10] J. Kliewer, R. Berndt, E. V. Chulkov, V. M. Silkin, P. M. Echenique, and S. Crampin, Science **288**, 1399 (2000).
[11] L. Bürgi, O. Jeandupeux, H. Brune, and K. Kern, Phys. Rev. Lett. **82**, 4516 (1999).
[12] L. Vitali, P. Wahl, M. A. Schneider, K. Kern, V. M. Silkin, E. V. Chulkov, and P. M. Echenique, Surf. Sci. **523**, L47 (2003).
[13] M. P. Everson, L. C. Davis, R. C. Jaklevic, and W. Chen, J. Vac. Sci. Technol. B **9**, 891 (1991).
[14] J. Li, W.-D. Schneider, and R. Berndt, Phys. Rev. B **56**, 7656 (1997).
[15] S. Crampin, M. H. Boon, and J. E. Inglesfield, Phys. Rev. Lett. **73**, 1015 (1994).
[16] S. Crampin and O. R. Bryant, Phys. Rev. B **54**, R17 367 (1996).
[17] S. Crampin, M. Nekovee, and J. E. Inglesfield, Phys. Rev. B **51**, 7318 (1995).
[18] S. Crampin, J. Kröger, H. Jensen, and R. Berndt, cond-mat/0410542 (unpublished).

[19] P. M. Echenique, R. Berndt, E. V. Chulkov, Th. Fauster, A. Goldmann, and U. Höfer, Surf. Sci. Rep. **52**, 219 (2004).
[20] P. M. Echenique and J. B. Pendry, J. Phys. C **11**, 2065 (1978).
[21] N. V. Smith, Phys. Rev. B **32**, 3549 (1985).
[22] A. Eiguren, B. Hellsing, F. Reinert, G. Nicolay, E. V. Chulkov, V. M. Silkin, S. Hüfner, and P. M. Echenique, Phys. Rev. Lett. **88**, 066805 (2002).
[23] P. Wahl, M. A. Schneider, L. Diekhöner, R. Vogelgesang, and K. Kern, Phys. Rev. Lett. **91**, 106802 (2003).
[24] S. Crampin, J. Kröger, H. Jensen, and R. Berndt, cond-mat/0410542 (unpublished).